Volume 4
Number 8
August 2025
Pages 1977-2274

Digital Discovery

rsc.li/digitaldiscovery

ISSN 2635-098X

ROYAL SOCIETY OF CHEMISTRY

PAPER
Maciej Haranczyk *et al.*
Streamlining material degradation testing: collaborative robotics for specimen monitoring

Digital Discovery

ROYAL SOCIETY OF CHEMISTRY

PAPER

View Article Online
View Journal | View Issue

Cite this: *Digital Discovery*, 2025, **4**, 2001

Streamlining material degradation testing: collaborative robotics for specimen monitoring

Brody Stack,[ab] Miguel Hernández-del-Valle,[ac] Alex Mascaraque-León,[a] Petronela Chovancová,[a] Loris Langeois,[ad] Jacob Porath,[ab] Juan P. Fernandez-Blazquez,[a] Mónica Echeverry-Rendón[a] and Maciej Haranczyk *[a]

The development of polymer materials for real-world applications requires careful assessment of material degradation over time and under environmental exposure. Such tests often necessitate frequent monitoring of test specimens, which can become burdensome for researchers. This study presents the application of a collaborative robot to automate repetitive tasks involved in monitoring materials exposed to solvents such as water. The primary setup enables the monitoring of a large number of specimens immersed in a water bath, recording their mass, and directing them for mechanical testing at specified intervals. The experiment is further supported by several do-it-yourself accessories, including Arduino-controlled water replacement, temperature regulation, and specimen drying. We demonstrate the setup's utility by monitoring water absorption in various nylon materials, as well as the Charpy impact strength of polylactic acid (PLA) specimens immersed in water. Lastly, we propose additional modifications to allow for more complex measurements, particularly for samples requiring precise control over the composition of the immersion solvent.

Received 15th January 2025
Accepted 14th June 2025

DOI: 10.1039/d5dd00016e

rsc.li/digitaldiscovery

1 Introduction

Polymer materials, particularly in the form of plastics, have become an essential component of modern life, symbolizing both technological progress and civilizational advancement. Their widespread use across diverse sectors—from consumer goods and healthcare products to advanced technologies—continues to drive the development of materials with enhanced performance, sustainable sources, and carefully designed degradation profiles. A crucial aspect of optimizing these materials involves the long-term monitoring of specimens to observe changes over time. The frequency of monitoring must align with the kinetics of the degradation process; however, more frequent testing can reveal valuable insights into the mechanisms and various stages involved. Traditional methods of manual testing are not only labor-intensive but also lead to scheduling challenges, particularly when tests are required during inconvenient times such as nights or holidays. In this study, we present the development of an automated experimental setup using a collaborative robot, aimed at streamlining and improving the efficiency of polymer material testing. Collaborative robots, also known as cobots, are a category of robots design to work beside alongside human workers and are tools of increasing popularity in the context of automated laboratories for their abilities to perform repetitive tasks while cooperating safely with the researchers.

One of the important aspects of polymer material monitoring is its degradation when exposed to moisture along with other factors such as temperature, oxidative stress, radiation, *etc.* Banjo *et al.*[1] investigated how common 3D printing polymers such as nylon and PLA degrade significantly when exposed to moisture and high temperatures over time, affecting their long-term use and recyclability. In their study, nylon-based materials absorbed up to 10 times more water than PLA, with nylon experiencing a 60% reduction in flexural modulus after 7 days of immersion, while PLA showed negligible degradation at 21 °C but substantial physical degradation at 70 °C.

Other studies have focused on the effect that different additives can have on the degradation of polymers. For example, montmorillonite is a nanoclay known for accelerating the processes of hydrolytic degradation and biodegradation of PLA.[2,3] Consequently, degradation becomes a critical factor to consider when using polymer nanocomposites. This effect may be detrimental in applications where resistance to environmental factors is required, but advantageous in cases where biodegradability is desired for end-of-life disposal. One relevant point about these processes of water absorption and degradation is that they are not linear and the polymers behave very differently in every stage of the process depending on which factor is dominant. Thus, regular monitoring is essential for

[a]*IMDEA Materials Institute, C/Eric Kandel, 2, 28906 Getafe, Madrid, Spain. E-mail: maciej.haranczyk@imdea.org; Tel: +34 915 49 34 22*
[b]*Michigan State University, East Lansing, 48824, MI, USA*
[c]*Universidad Carlos III de Madrid, 28911 Leganés, Madrid, Spain*
[d]*Université de Limoges, 87032 Limoges, France*

achieving a profound comprehension of the phenomena at play. Moetazedian *et al.*[4] performed this type of detailed study in the context of 3D printing PLA for biomedical applications and described how at early stages the loss of crystallinity is the main factor affecting the mechanical properties, while in later stages the dominant process is the hydrolysis of the polymer chains. They also characterized how the degradation times change dramatically corresponding to temperature, with the polymer reaching zero tensile strength at 270 days if submerged at 37 °C, while only taking 4 days if the water is at 65 °C. In this context, the advantage of automation is clear, as it allows for systematic measurements in processes that happen in just a few hours without interruptions related to work schedules.

The need for automated polymer material testing extends beyond degradation studies, encompassing broader applications in the research and development of advanced materials. Various groups have pioneered systems for high-throughput and automated testing to address this demand. For instance, the Meredith group introduced the HTMECH device,[5] designed for high-throughput screening of thin films. This system measures force and deformation in film regions subjected to transverse biaxial loading through an instrumented thin contact tip. Specifically tailored for rapid serial testing of combinatorial material libraries, HTMECH processes discrete or gradient samples, each with a diameter of only a few millimeters, collecting load-deformation profiles at high speeds (*e.g.*, 100 spots per hour). Similarly, the Brown group developed the BEAR system,[6] which automates the optimization of mechanical properties of 3D-printed structures. This setup integrates a universal testing machine from Instrom with a collaborative robot, which facilitates the mechanical testing of 3D-printed materials. Our own group has previously reported an automated system for optimizing 3D printing parameters, incorporating both a collaborative robot and automated mechanical testing using a Charpy pendulum tester, coupled with computer vision for quality control.[7] The importance of such automated testing systems is widely acknowledged by both researchers and instrument manufacturers, with the latter offering instruments featuring automated sample loading or integration with collaborative robots through proprietary solutions.

In this study, we extend the application of collaborative robotics to automate repetitive tasks involved in monitoring polymer materials exposed to solvents such as water. This is particularly critical for developing sustainable polymers and materials that are used in biomedical applications. Our primary setup enables the monitoring of numerous specimens immersed in a water bath, facilitating mass measurements and directing the samples to mechanical testing at predefined intervals. The system is enhanced with several custom-built accessories, including Arduino-controlled water replacement, temperature regulation, and specimen drying. The utility of this setup is demonstrated by monitoring water absorption in various nylon materials, as well as the Charpy impact strength of PLA specimens immersed in water. In addition, we discuss potential modifications for more complex measurements, especially for specimens requiring precise control over the composition of the immersion solvent.

2 Methods

2.1 Experimental setup for water immersion experiment

The complete experimental setup is presented in Fig. 1A. The immersion of test specimens takes place in a Fisherbrand™ Isotemp™ FSGPD28 general purpose water bath. To record the weight of the specimens during the experiment, a Gibertini CRYSTAL 500 CAL CE/C is used. A UR10e collaborative robot from Universal Robots is tasked with transporting the samples from the water bath to the balance and *vice versa* while a number of additional accessories facilitate the experiment. In the following subsections, the different components of the setup are described in further detail.

2.1.1 Experiment workflow. The whole robotic workflow is implemented through Python scripts, which facilitate maintenance and scalability. The user can easily change the parameters of the experiment depending on the number of specimens, the length and number of the cycles, *etc.* These modifications can be made through a JSON configuration file, eliminating the need to alter the underlying Python code. This approach simplifies customization and minimizes the likelihood of introducing errors. The process works as follows:

(1) At the beginning of each cycle, the robot removes the lid from the water bath that prevents excessive evaporation or external contamination and stores it by the side of the water bath (Fig. 1A-2).

(2) After the lid is removed the tool is returned to initial position, as seen in Fig. 1A, and a calibration routine is performed to accurately establish the position of the water bath with respect to the robot coordinate system, as detailed in Section 2.1.4.

(3) Once calibrated, the robot follows the grid of samples and pulls each in the order they are called under the user inputs section.

(4) Each sample is retrieved from the tray and moved to a location to be dried with compressed air (Fig. 1B-7). The specimen is administered two bursts of compressed air through a custom robot gripper, described in Section 2.1.3. These are set to 1.5 seconds each but can be adapted as material requires.

(5) The air-dried sample is then moved to the sponge (Fig. 1B-8) where its bottommost face is dabbed to remove any remaining drops. After using the sponge, the sample is moved to the balance (Fig. 1B-9) to be measured.

(6) Each sample is measured three times so that an average can be taken for improved accuracy. Together, all four values are reported along with a timestamp and the current temperature of the bath. This data is added to that sample's data category.

(7) After measurement, the sample is returned to the water bath tray and re-submerged. Once all desired samples have been measured, the lid is replaced over the bath. It is at this point that data is saved and added to the experiment's CSV file.

The robot then waits until the current time matches that of the previously calculated next cycle time. In order to improve unsupervised compliance, special procedures were created for

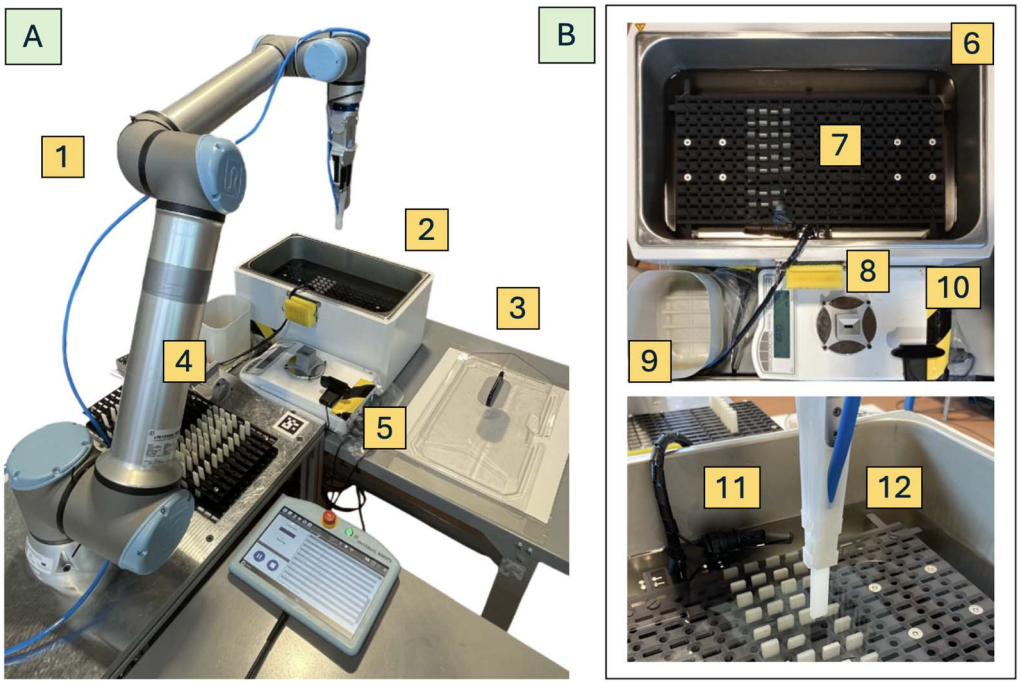

Fig. 1 Setup for testing environment. Diagram A shows the full setup while diagram B depicts the alignment of adjacent testing equipment. Components are as follows; (1) UR10e robot arm, (2/6) Isotemp water bath, (3) lid storage during testing, (4/9) receptacle for air drying, (5/10) Gibertini crystal balance, (7) 3D printed tray, (8) kitchen sponge, (11) water level sensor, (12) 3D printed gripper.

each way the grippers interact with a sample. They are as follows:

(a) Basin tray retrieval: grippers are lowered fully opened, closed slightly so that the angled teeth start to control the sample, shaken along the X–Y plane to further center the substrate, and then closed fully.

(b) Basin tray replacement: the sample is lowered most of the way down so that it interacts with both the tray and robot, the grippers open slightly to drop a sample in the case it is already perfectly aligned, the tool is then lowered the rest of the way down, shaken along the X–Y plane to help the sample settle.

(c) Balance placement: the sample is lowered most of the way down so that it interacts with both the balance and robot and the grippers are opened to their full width to avoid interference with the measurement, then the tool is rotated +30 and back −30° about the Z axis to free a sample in the case that it was stuck to the grippers.

(d) Balance retrieval: grippers are lowered fully opened, closed slightly so that the angled teeth start to control the sample, shaken along the X–Y plane to further center the substrate, and then closed fully.

To enhance scalability, the system has been extended to support parallel execution of multiple experiments. A second water bath has been integrated, allowing two independent experiments to run simultaneously. This is achieved using a queue-based architecture implemented in Python, where a listener manages incoming tasks and distributes them to one or more clients that execute the experimental routines. Each bath operates as a fully autonomous unit, enabling asynchronous and decoupled operation. This design not only doubles the throughput but also lays the groundwork for future expansion—the system can be scaled further by adding additional baths, limited only by physical space and available hardware. The codebase supporting both single-bath and multi-bath configurations is included in the GitHub repository for this project.[8]

2.1.2 Water bath and tray design. To hold samples during testing a four-layered tray was designed to allow for water circulation while maintaining a tight tolerance on the substrate's position. This was achieved by adding large bevels to the lower layer so that when released, a sample would naturally settle to the center. The larger submerged tray also features small bevels on the upper layer to aid in the case that a sample experiences warping during testing. The interface between the robot and the balance also uses this geometry, although it is more robust and enclosed for better stability.

Situating substrates vertically in a self-centering tray allows for many samples to be placed in a tight pattern. The current arrangement of 23 columns by 11 rows, 2 cm on center, provides 253 potential samples in any one experiment.

Due to the water immersion and high temperatures of the bath, ASA was selected as the material for fabricating the basin tray. ASA resists degradation in this type of environment, while allowing for the beveled geometry originally designed for 3D printing. Exterior trays and other robot interfaces are 3D printed in PLA as they will not be subjected to as harsh of environments. The CAD files for the tray and all components can be found in the GitHub repository for this project.[8] There are two versions: one for rectangular specimens apt for Charpy impact

testing and another one adjusted for tensile dogbones according to the ISO 527-2 norm.

2.1.3 Robot gripper design. The robot's end effector for this experiment was designed to achieve three specific tasks: control a vertically oriented polymer sample, interface with the water bath lid, and dry each sample after immersion in the bath. Many iterations were tested before arriving at the current design, which gave rise to the features pictured in Fig. 2. The CAD files for the gripper can be found in the GitHub repository for this project.[8]

Offset teeth on each gripper interlock with those of its pair to better control sample acquisition. The geometry of the combined two grippers pushes the sample towards the tool's center as the grippers close. Due to the axially symmetric nature of this pattern, the same design can be used for both sides. This feature is aided by a function which wiggles the tool slightly along the *X*–*Y* plane before fully closing the grippers. Together, these features allow for the compliance necessary to be left unattended for multiple days.

Included in the geometry of the teeth is a circular cutout which is designed to interface with the bath lid handle. The *X*–*Y* cross section constrains a sample to one point along this plane, while the *Y*–*Z* cross section constrains the lid's handle to one point on this plane. This small amount of geometry provides reliable control over the movement of two unique parts of the robot's environment.

The channels along the inner face of the gripper are connected to a system of compressed air to assist in drying each sample before measuring its weight. Removing surface water and any water trapped between the gripper and sample is crucial to the accuracy of the results collected, especially as it is to be left unsupervised. Funneling compressed air to run out along each face of a controlled sample solves both concerns. Fig. 2 shows a cross-section view of a gripper which depicts the air channels in yellow and the mounting for the UR10e robot in green. The air channeling consists of a press-fit hole for inserting 8 mm OD pneumatic tubing which is then divided into a channel that runs along the inner control surface and a smaller duct that directs air out towards the end of a held sample. After use of compressed air, the bottom face of the sample is dabbed on a sponge and each side is passed along it downward, removing any remaining drops from both the sample and the grippers.

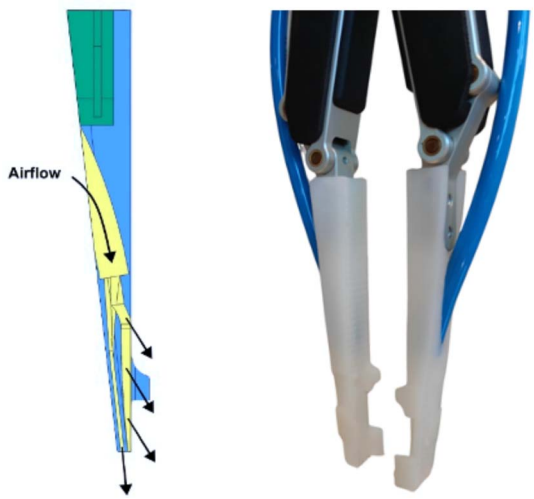

Fig. 2 End effector for UR10e robot arm with channeling for compressed air. On the right, schematic view of the gripper (blue) with the air circulation channels (yellow) and the robot mounting (green). On the left, 3D printed grippers mounted on the robot connected to 8 mm OD pneumatic tubing.

Another important consideration is fabrication, especially for a piece with such complex geometry. For this reason the outer face of each gripper is planar so that it lays flat on a 3D-printer build plate. This minimizes support material, printing time, and post-print modifications. The triangular shape also yields better rigidity, which is helpful since the depth of the water bath requires that the grippers have some distance between the point of actuation and their point of contact with the substrate.

2.1.4 Collaborative robot interface. The UR10e collaborative robot is controlled using `ur-rtde`[9] library for real-time control. This library has capabilities for programming the robot movements, getting feedback about position or force, and operating the robot grippers by using the I/O interface.

The location of each item the robot will interface with is calculated from one initial position, where the robot is directly above the water bath's lid. All adjacent equipment is in contact with each other to maintain consistent relative positions between devices, as depicted in Fig. 1 for this workflow.

After the lid has been removed, the robot uses force-contact feedback to detect two points along the *X* axis and two along the *Y* axis. These points are converted into lines and a point of intersection is calculated for the corner of the bath. If the two lines are not within a certain tolerance of perpendicularity (*i.e.* if there was outside interference during this process), the calculation is rejected and the function restarts until a precise measurement is validated. Once the alignment data satisfies the set tolerance, the experiment environment is calculated using distances from the corner point of intersection and the angle of the lines off the robot's origin.

Coordinates are calculated using the rotation matrix with inputs initial position (X_i, Y_i), angle (α), and position of the specimen in the tray (dx, dy) in the following format:

$$X_n = X_i + dx \cdot \cos(\alpha) - dy \cdot \sin(\alpha)$$

$$Y_n = Y_i + dy \cdot \cos(\alpha) + dx \cdot \sin(\alpha)$$

The position of each specimen in the tray (dx, dy) is defined by assigning an integer index (nth column, nth row) and multiplying by the 2 cm between the center of the cells.

This system allows for variability in setup and during the experiment. Including the calibration at the start of every cycle greatly decreases the chances of failure over long periods of unattended testing.

2.1.5 Peripheral devices. The balance is connected to a Raspberry Pi 4 through a RS-232 port and USB adapter, while

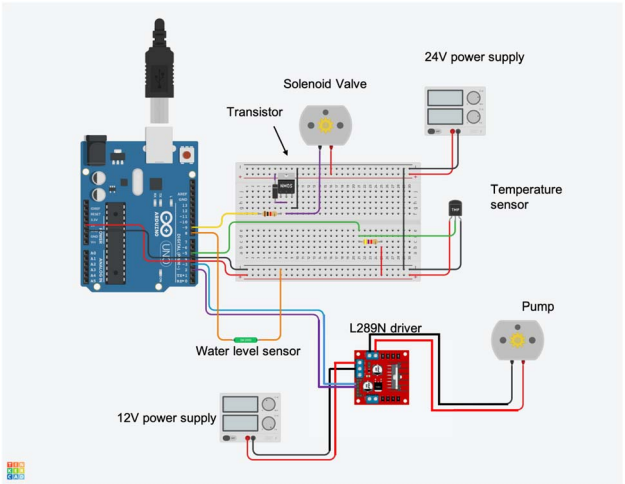

Fig. 3 Arduino and circuit to manage the peripheral devices.

Fig. 4 Polyamide specimens used in water absorption experiment.

the communication is handled with the `pyserial` library and functions to read measurements, tare and calibrate. The communication between the main computer and the Raspberry Pi takes place through socket connection, so it is possible to send commands and receive measurements.

The same socket protocol is used to communicate with an Arduino board connected to the Raspberry Pi, which controls a series of devices that ensure the proper functioning of the experiment (Fig. 3):

A 12 V DC water pump is controlled by an Arduino UNO and maintains a constant water level in the bath throughout the experiment. A float switch water level sensor placed inside the bath sends information on water conditions using the `pyserial` and allows for the automatic activation of the pump if it detects an insufficient water level. A driver (L289N) is used to supply the pump with 12 V.

Additionally, a temperature sensor with a waterproof probe is immersed in the bath to monitor water temperature throughout the experiment. A pull-up resistor (4.7 kΩ in the case of the sensor used here) is needed to ensure correct data communication between the various devices.

The compressed air valve used to dry each sample after immersion is also controlled by the Arduino. This setup calls for a 24 V power supply, requiring the use of a second power source. To correctly connect it to the Arduino, a MOSFET type transistor is needed; a resistor (1 kΩ in this case) to limit the current flowing through the transistor, and a freewheeling diode to protect it from experiencing too high of voltage.

All the commands can also be read or sent by Python from a single interface.

2.2 Materials and specimen production

For experiments studying PLA degradation, we used PLA Ingeo 4043D from NatureWorks. PLA was extruded using a co-rotation twin-screw extruder 16 mm with L/D ratio of 30 at 200 °C with a screw speed of 100 rpm. The specimens were injected using a Babyplast 6/12 Standard microinjector at 200 °C and 90 bar. The specimen shape is a rectangular prism of 80 × 13 × 3.2 mm with slightly rounded corners for better ejection. The PLA was dried overnight at 45 °C before injection.

For the experiments of water absorption of polyamides, a number of different formulations were used to compare their behaviours. Also, depending on the material, some of the specimens were 3D printed (-P) and some were injected (-I) according to the way in which the material is commercialized. The specimens were printed at 100% infill and with the same geometry as the injected specimens.

(a) bioPA56-I: ECOPENT®1273 Bio-based Polyamide Resin PA56 from Cathay Biotech Inc were injected at 260 °C and 32 bar.

(b) BASF Ultrafuse PA (PA6-I and PA6-P), a PA6 and PA66 copolymer with reduced melt temperature. The filament was both 3D printed in a Bambu X1 Carbon printer at 240 °C, and injected at 220 °C and 90 bar to compare absorption in both methods.

(c) Fiberlogy PA12 natural filament (PA12-P) printed at 300 °C. PA12 is expected to have lower absorption rates than other polyamides.[10]

(d) Fiberlogy Recycled PA12 filament (rPA12-P) printed at 300 °C, which offers an interesting point of comparison with its non-recycled counterpart.

The specimens are shown in Fig. 4.

To test the effect of water adsorption on the mechanical properties of PA, we also injected 50 samples of bioPA56 tensile dogbones. The specimens were injected at 260 °C and 32 bar.

2.3 Testing methods

The impact strength testing is performed with a Zorn Stendal Pendulum Impact tester with a capacity of 4 J, which was automated with a UR5 collaborative robot from Universal Robots and aided by camera vision systems and Arduino controllers, as described in a previous article from our group.[7]

Tensile tests were conducted in accordance with ISO 527-2 using an Instron universal testing machine equipped with a 10 kN load cell. The crosshead speed was set to 50 mm min^{-1}. Specimens had a gauge length of 25 mm, thickness of 2 mm,

and width of 5 mm. Each measurement was performed in triplicate.

Thermal transitions were studied by differential scanning calorimetry (DSC) using a TA Instruments DSC25 in a heating–cooling–heating cycle at a rate of 10 °C min^{-1} under a nitrogen atmosphere. Samples were first equilibrated at −20 °C, then heated to 200 °C, held isothermal for 0.5 minutes, cooled to −20 °C, held isothermal for 1 minute, and finally reheated to 200 °C. Data from the first heating cycle were used for thermal analysis to assess the material in its initial state.

3 Results and discussion

3.1 Absorption experiment with polyamides

In this experiment, specimens from the 5 different polyamides mentioned in Subsection 2.2 were submerged in demineralized water at two temperatures: room temperature (that was measured to be 22.6 ± 0.6 °C during the experiment) and 60 °C. The specimens were extracted, dried and weighed every 3 hours, and then placed again in the water bath.

The evolution of the weight of the specimens is shown in Fig. 5. The PA12 specimens, both recycled and non-recycled, show a lower weight and almost no absorption (≤1.2%) at both temperatures, while all the other specimens have similar weights and absorption rates, as calculated in Table 1:

At both temperatures, bioPA56 is the material that shows faster absorption, but this rate is greatly increased with exposure to higher temperature. The samples of PA6 show very similar trends, with no noticeable difference between the 3D printed and the injected samples.

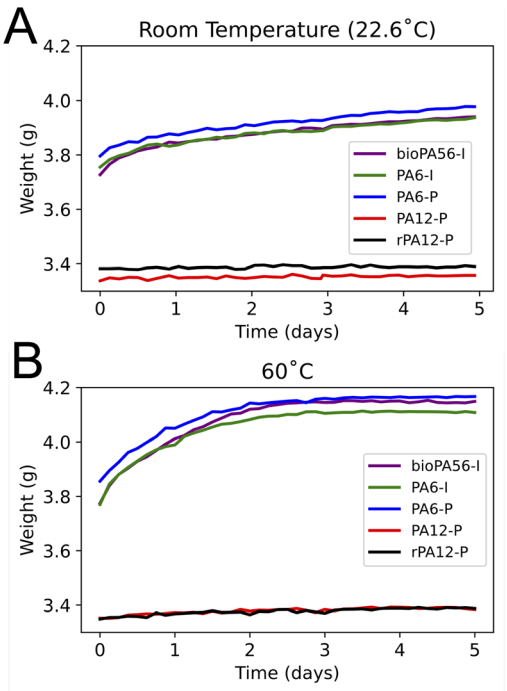

Fig. 5 Evolution of the weight of the polyamide specimens at (A) room temperature and (B) 60 °C.

Table 1 Difference between initial and final weight of the specimens submerged at room temperature and 60 °C after 5 days of immersion

Material	%wt at room T	%wt at 60 °C
bioPA56-I	5.82	9.76
PA6-I	4.88	8.55
PA6-P	4.82	8.20
PA12-P	0.60	1.20
rPA12-P	0.33	1.09

The marked difference in water absorption between PA12 (both virgin and recycled) and the other polyamides tested corroborates previous findings.[11,12] This reduced water uptake in PA12 is primarily attributed to its lower density of amide groups; PA12 features only one amide group per 12 carbon atoms, compared to a ratio of 1 : 6 in PA6 and PA66 and 2 : 11 in PA56.[13,14] Given the strong affinity of amide groups for water, owing to their polarity, water molecules can induce a plasticizing effect by disrupting inter-chain hydrogen bonding, thereby increasing molecular mobility.[15,16] Consequently, to limit moisture absorption while preserving the mechanical properties characteristic of PA6, PA6/PA12 copolymers are frequently employed in applications where water uptake must be controlled.[17] Additionally, the degree of crystallinity influences water absorption, as moisture predominantly penetrates the amorphous regions of the polymer.

3.1.1 Mechanical testing of PA. To have a more complete view of the effect of water absorption on the mechanical properties of the material, we injected 50 tensile specimens of the material that showed greater absorption, in this case bioPA56.

Fig. 6 shows the sharp initial drop in Young's modulus and yield strength after just one day, suggesting rapid chain scission, most likely driven by water interaction with the amide groups. This degradation may be further accelerated by oxidative mechanisms. As highlighted by Brette *et al.*, the presence of oxygen, both from air and dissolved in water, introduces oxidative degradation. Thermal oxidation, initiated by hydrogen abstraction on the aliphatic backbone, accelerates polymer

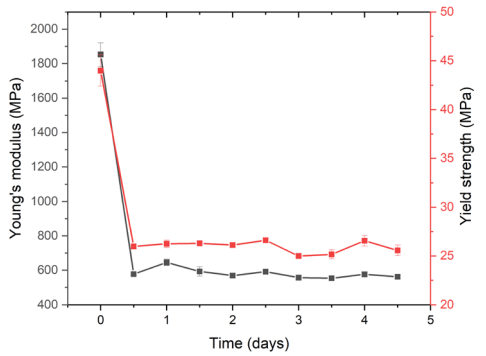

Fig. 6 Evolution of Young's modulus (black, left axis) and yield strength (red, right axis) of PA during hydrolytic degradation at 60 °C over 4.5 days.

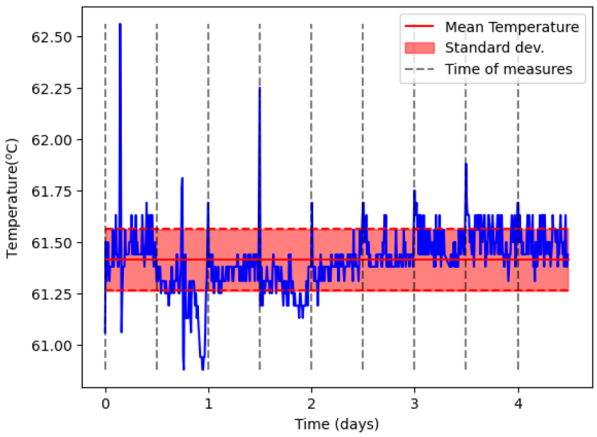

Fig. 7 Temperature profile during the experiment as measured by the submerged temperature probe.

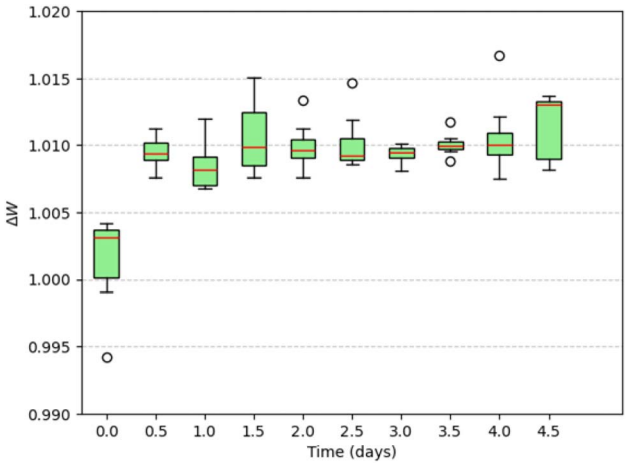

Fig. 9 Weight increment measurements of the PLA specimens at 60 °C. Every 12 h, 10 specimens are retrieved, weighed and stored for mechanical testing.

breakdown and leads to irreversible structural changes such as embrittlement and possible cross-linking.[18]

The temperature profile of the water during the experiment is shown in Fig. 7. Temperature stays close to the 61.41 °C mean with a 0.15 °C standard deviation. Most of the biggest deviations match with the times where the lid is removed to measure the weight of the specimens, causing the temperature to drop slightly and requiring the bath to heat in order to recover the target temperature. Another possible cause for temperature variation could be the process of refilling water when the level drops below the sensor.

3.2 PLA degradation experiment

For this experiment, PLA Ingeo 4043D from NatureWorks was extruded and, subsequently, 100 specimens were injection molded and submerged in the water bath at 60 °C, which is approximately the glass transition temperature for the material.[19] The specimens were weighed before immersion to have a reference value with which the change in weight can be compared. This is expressed as $\Delta W(t) = W(t)/W_{\text{ref}}$.

Every 12 hours, 10 specimens are extracted from the water bath, dried with two 1.5 second bursts of compressed air, weighed and stored for subsequent mechanical testing. Fig. 8A shows the initial setup of the specimens. The experiment runs for 4 and a half days until all of the samples are extracted from the water or the degradation is so noticeable that it is no longer possible to keep conducting the experiment due to the specimens breaking on touch. A first effect that can be easily observed in Fig. 8B is the progressive loss of transparency until samples are completely opaque after around 72 h, due to the polymer crystallization. During early prototyping, we noticed that some samples acquire a curvature (see Fig. 8C for an example) which creates difficulties when trying to insert them into the balance fixture. In order to prevent this, our improved design uses three layers of trays and smaller tolerance in the holes to help maintain the shape during the experiment.

The samples' weights, measured every 12 hours for 4 and a half days, are shown in Fig. 9. An increase in weight of around 1% can be observed in the first hours of the experiment, after which the weight becomes very stable. This value of water absorption for PLA close to 1% agrees with that which is previously reported in literature.[1] On the other hand, no

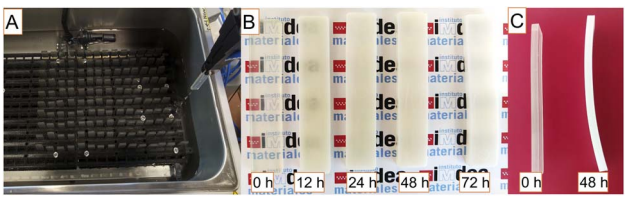

Fig. 8 Setup and visual results of the PLA degradation experiment. (A) Initial setting of the PLA specimens in the water bath. (B) Specimens removed at different points of the experiment. The PLA degradation causes a progressive loss of transparency. (C) Shape of different specimens. After some time submerged, the initially straight specimens frequently show a curvature that causes problems when trying to insert them into the balance fixture.

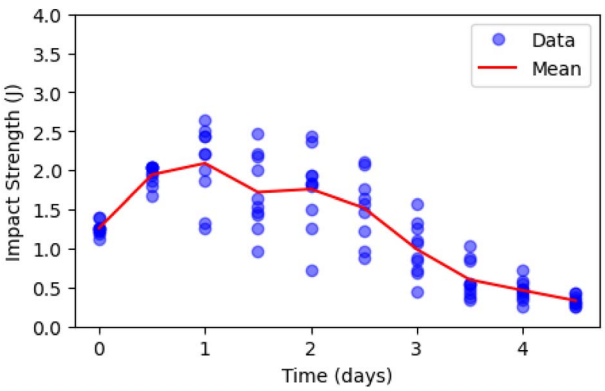

Fig. 10 Impact measurements of the PLA samples performed every 12 h at 60 °C.

decrease in weight associated to degradation is perceived, as the PLA chains broken by hydrolysis typically remain in the material[20] and do not affect the overall weight change of the specimen.

3.2.1 Mechanical testing of PLA. Tests were conducted on the specimens that had been submerged at 60 °C and retrieved every 12 h, as shown in Fig. 10. This process exhibits distinct phases. In the first 24 hours, impact strength increases significantly, likely due to the plasticizing effect of water and elevated temperature. From days 1 to day 3, mechanical strength gradually declines, with considerable variability between specimens. This inconsistency may result from differences in the extent of plasticization and molecular weight degradation across samples.[4] After day 3, variability diminishes, and the mechanical properties continue to deteriorate until the material becomes so fragile that it fractures upon handling.

To understand the significant variability in impact strength, we performed DSC analysis on samples degraded for 0.5 days (low variability) and 1 day (high variability). The analysis was based on the first heating curve, which reflects the material's thermal state after degradation. Fig. 11 presents the DSC thermograms, with corresponding numerical data summarized in Table 2.

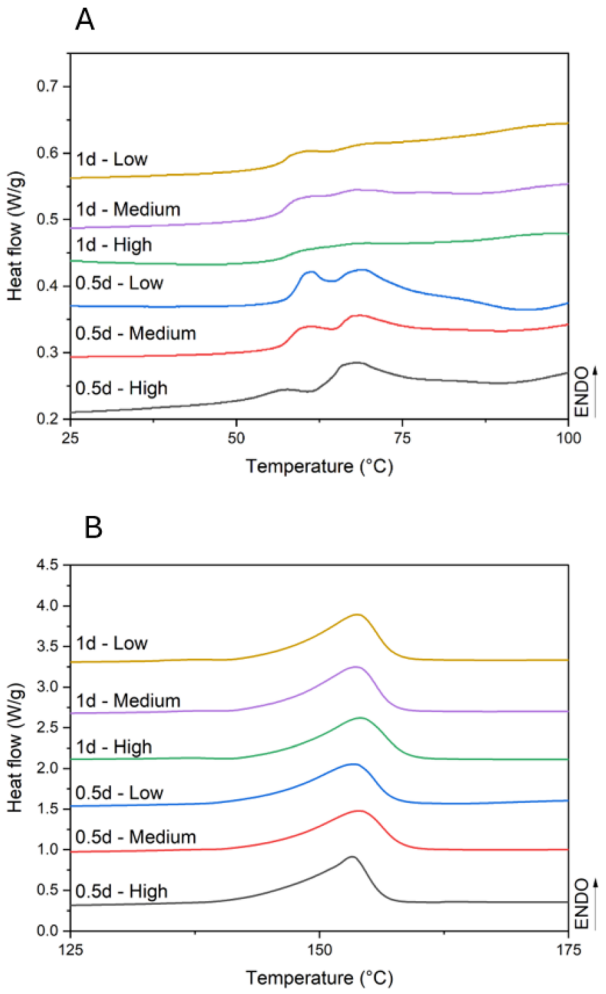

Fig. 11 DSC thermograms (first heating curve) of injection-moulded PLA samples hydrolytically degraded in water at 60 °C for 0.5 day (0.5 d) and 1 day (1 d). Samples are categorized by impact strength level (high – highest value obtained, medium – medium value, low – lowest value obtained). (A) Glass transition temperature region (B) melting temperature region.

Table 2 Summary of measured impact strength, glass transition temperature (T_g), and enthalpy of melting (ΔH_m) of samples submerged for 0.5 day and 1 day in water at 60 °C. Samples are categorized by impact strength level (high – highest value obtained, medium – intermediate value, low – lowest value obtained)

Sample	Impact strength (J)	Glass transition (60 °C)	ΔH_m (J g^{-1})
0.5 d – high	2.04	63.09	28.66
0.5 d – medium	1.79	57.90	28.59
0.5 d – low	1.68	58.83	25.31
1 d – high	2.64	56.40	27.31
1 d – medium	1.86	57.46	29.45
1 d – low	1.26	56.23	29.47

At 0.5 day, impact strength values remained relatively consistent across samples, indicating a uniform effect of water diffusion limited mostly to the surface. In contrast, after 1 day, impact strength showed substantial variation. This increase in variability suggests that as water penetrated deeper into the polymer, it interacted differently with the material's microstructure, depending on local variations in crystallinity, porosity, or chain entanglement. While the samples exhibited a decrease in glass transition temperature after 24 hours indicating increased chain mobility due to water-induced plasticization, the enthalpy of melting (ΔH_m) showed an inverse trend compared to impact strength. After 12 hours, ΔH_m values decreased with decreasing impact strength. However, after 24 hours, ΔH_m increased in samples with decreasing impact strength. This is consistent with literature, indicating that hydrolytic cleavage occurs preferentially in the amorphous regions, leading to an increase in overall crystallinity.[21]

To gain a better understanding of kinetics of the process, the experiment was repeated at a lower temperature of 50 °C as shown in Fig. 12. However, in this case, the material preparation differed, as the PLA was directly injection molded, bypassing the extrusion step. In this case, a sustained increase in the mechanical strength of the specimens was observed, without reaching the point where degradation becomes dominant and they become more fragile. The data variability is evident in the case of 50 °C degradation as well, with increased scatter appearing around day 2. At 60 °C, however, variability begins as early as day 1. This observation is consistent with the general principle described by the Arrhenius theory, where higher temperatures accelerate chemical reactions. However, it is crucial to note that at 60 °C, the PLA is above its glass transition temperature (T_g), unlike at 50 °C. This difference in physical state significantly increases polymer chain mobility, which likely enhances the acceleration of degradation processes beyond the typical Arrhenius prediction.

3.2.2 Comparison with manual testing. To address the high variability observed—particularly in the impact testing

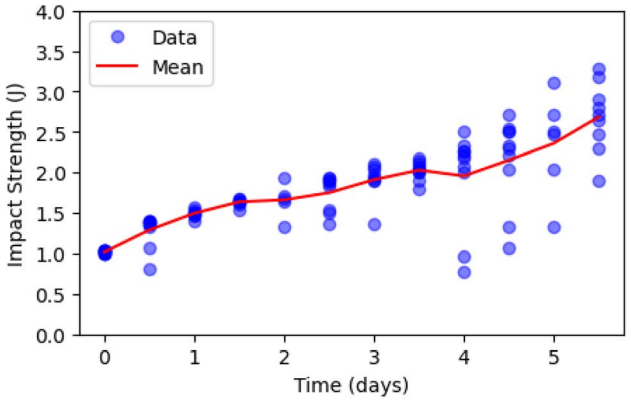

Fig. 12 Impact measurements of the PLA samples performed every 12 h at 50 °C.

experiments—manual measurements were conducted on PLA specimens conditioned at 60 °C. These tests were performed every 24 hours and were intended to serve as a comparison with the results obtained using the automated system (the same time points shown in Fig. 9 and 10). The outcomes are presented in Fig. 13.

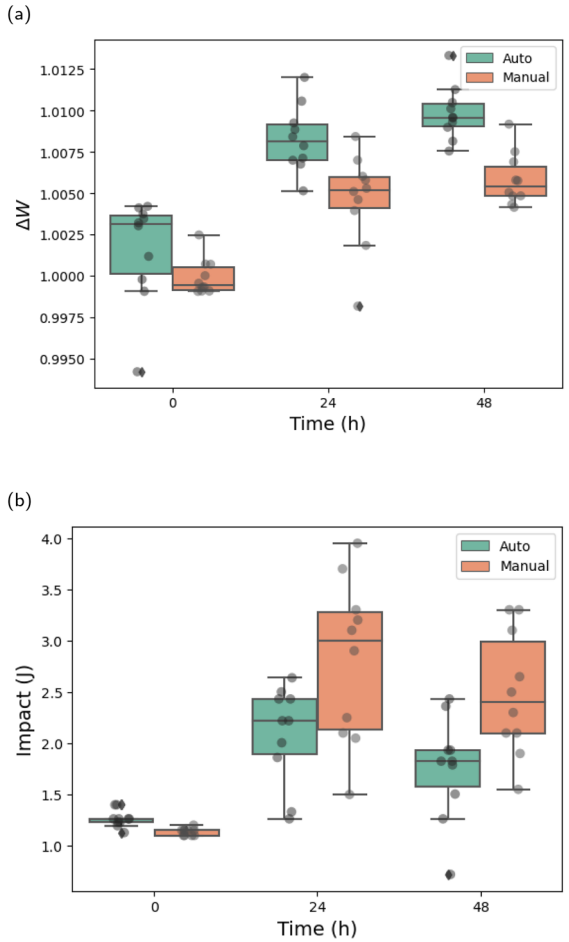

Fig. 13 Comparison between measures taken automatically and by hand for (a) weight change and (b) impact strength.

For the weight change measurements (Fig. 13a), the variability in manually measured data is comparable to that of the automatic system. The average standard deviation was 0.0019 for manual measurements and 0.0024 for automated ones, indicating similar levels of dispersion. Interestingly, the manually recorded mean values are consistently slightly lower than those obtained from the automated setup, although the overall trend remains the same. This discrepancy may be due to a delay between sample removal from the bath and weight measurement in the manual procedure. Unlike the automated system, which measures the weight immediately after drying, the manual samples had a few additional hours of drying time. This could have led to further evaporation and, consequently, a reduction in measured weight due to the loss of some absorbed water.

For the impact testing results shown in Fig. 13b, the variability was noticeably higher in the manually conducted experiments. This highlights a key advantage of automation: reducing human-induced inconsistencies. In particular, the automated system ensures more repeatable and consistent sample placement, which likely contributes to the lower variability observed. The average standard deviation decreased from 0.47 J in the manual tests to 0.35 J with the automated setup. Another limitation of manual testing is its reduced flexibility in scheduling measurements. Due to working-hour constraints, manual tests could only be performed every 24 hours, whereas the automated system allowed for more frequent testing—every 12 hours—as shown in Fig. 9 and 10. This increased temporal resolution enables a more detailed understanding of the material's behavior over time.

4 Proposed adaptations

The experiments discussed thus far focus on regularly shaped substrates immersed together in one water bath. As a variation of the experiment, we designed a version for a case in which the samples have to be submerged in individual vials, where said vials are placed in the water bath to regulate their temperature. This is standard practice if the medium is a liquid other than water (*e.g.* simulated body fluid) or it is necessary to avoid cross-contamination between specimens.

In order to hold the test tubes in place, a vial tray was designed to keep the tubes upright, as seen in Fig. 14A2. A PLA ring was added near the base of each tube which allows it to interlock with the holder. This external holder allows for interaction with the cap to each vial, shown in Fig. 14B. Once the vials are inserted into the holder, the robot tool rotates counterclockwise and the PLA ring locks into place, enabling robot to remove the TPU corks that seal the tubes so that the material or liquid inside can be tested or replaced.

An automated syringe (Fig. 14A1) was adapted from Yoshikawa *et al.*[22] to extract and add liquid to the vials. This allows replenishing of the liquid to keep the level constant, replace it periodically if needed or correct the pH with buffer solutions, among other functions. The syringe is programmed on an Arduino UNO, which is integrated into the workflow using Python and can dispense up to 20 milliliters at a time. Similarly,

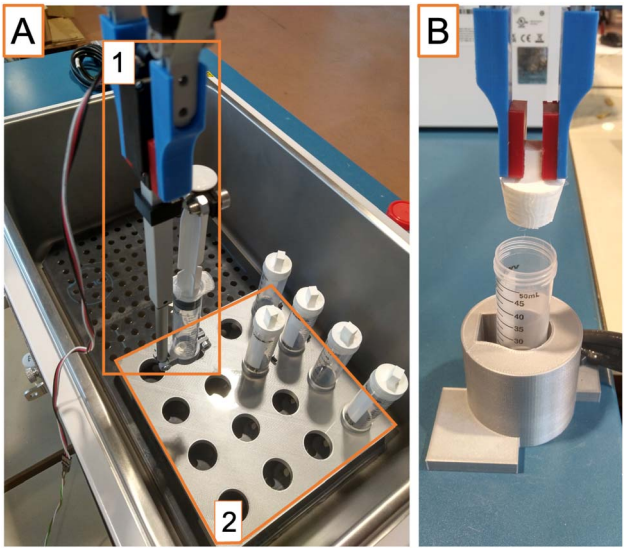

Fig. 14 Setup for vial experiment: (A) image of the water bath with syringe (1) held by the robot and the tray (2) for arranging the vials, each of them capped with a TPU cork. (B) Capping station designed for placing and removing the corks.

the collaborative robot can be programmed to measure additional parameters such as pH of the solution, in cases where these parameters are of importance to specimen degradation. Such a pH probe could also be monitored by an Arduino controller. The designs and Arduino code for the prototype are available in the GitHub repository of the project[23] for adaptation and future development.

5 Conclusions

This study demonstrates the significant benefits of using collaborative robotics to automate the repetitive tasks involved in monitoring materials exposed to environmental conditions, such as immersion in water. By automating specimen handling, mass measurement, and mechanical testing, our approach greatly reduces the burden on researchers, allowing them to focus on data analysis and experimental design rather than labor-intensive manual tasks. The integration of do-it-yourself accessories, including Arduino-controlled water replacement, temperature regulation, and drying systems, further enhances the versatility and reliability of the setup. Furthermore, our automated setup allows for seamless identification of important changes to the monitored specimens, allowing to focus further experimental resources on characterization of such to unveil degradation mechanisms. The automated system also improves consistency and enables higher-resolution data collection by reducing the human-induced variability in the results.

In the experiments performed to validate the setup, we studied the behavior of PLA and several grades of PA when immersed. In the PA experiment, the most notable results were the important increase in water absorption at 60 °C compared to room temperature, and the greatly reduced absorption of PA12, both neat an recycled, compared to the other formulations tested. Tensile testing of the formulation that showed higher absorption exhibited a noticeable decrease in both Young modulus and yield stress after just 12 h of immersion, after which it becomes stable. In the case of PLA, absorption was close to 1% and the experimental setup was used to collect specimens for impact testing. With the specimens submerged at 60 °C we observed a first phase of plasticization of the material that increases the resistance to impacts, which is later decreased by the degradation of the material until its resistance is negligible. DSC analysis was performed on some of the specimens to gain insights into the effect of water in the microstructure of the polymer.

Our approach provides a flexible framework that can be readily adapted for various material degradation studies. The system's modular design enables easy modifications, making it suitable for more complex experimental protocols that require precise control over environmental variables, such as the composition of the immersion solvent. This adaptability is particularly valuable for studies involving degradable materials, such as those used in tissue engineering, where maintaining specific conditions is crucial for replicating real-world scenarios.

In summary, the use of collaborative robots not only streamlines repetitive experiments but also opens new opportunities for customized testing setups, fostering innovation in the development and assessment of advanced materials.

Data availability

The STL files, electrical schemes, and software related with the project are deposited in an open access GitHub repository referenced in the article (**https://github.com/AMDatIMDEA/PolyMersion**, DOI: **https://doi.org/10.5281/zenodo.15658192**). Furthermore, the files related with the experimental setup extensions discussed in the manuscript are collected in another repository (**https://github.com/AMDatIMDEA/WaterBathExperiments**, DOI: **https://doi.org/10.5281/zenodo.15657923**).

Author contributions

B. S., M. H.-d.-V. and A. M. L. developed the core of the automated testing setup, comprised of software for robot operations and designs for all robot – sample interfaces in the testing environment. L. L. developed the Arduino control system. P. C. performed polymer characterization experiments. J. P. contributed to the extension for precise control of immersion experiments. M. H.-d.-V. and A. M. L. prepared the material specimen and collected the final results. J. P. F.-B., M. E.-R. and M. H. conceptualized the project. M. H. supervised the project and acquired funding. All authors contributed to the writing of the manuscript.

Conflicts of interest

There are no conflicts to declare.

Acknowledgements

We acknowledge the support from the MAD2D-CM project on Two-dimensional disruptive materials funded by the Community of Madrid, the Recovery, Transformation and Resilience Plan, and NextGenerationEU from the European Union. Additionally, B. S. and J. P. were supported by the National Science Foundation Division of Material Research (Grant No. DMR2153316) through the International Research Experience for Students (IRES) program.

References

1 A. D. Banjo, V. Agrawal, M. L. Auad and A.-D. N. Celestine, *Compos., Part C: Open Access*, 2022, **7**, 100243.
2 K. Fukushima, C. Abbate, D. Tabuani, M. Gennari and G. Camino, *Polym. Degrad. Stab.*, 2009, **94**, 1646–1655.
3 K. Fukushima, D. Tabuani, M. Arena, M. Gennari and G. Camino, *React. Funct. Polym.*, 2013, **73**, 540–549.
4 A. Moetazedian, A. Gleadall, X. Han, A. Ekinci, E. Mele and V. V. Silberschmidt, *Addit. Manuf.*, 2021, **38**, 101764.
5 D. Shoukat, J. T. Rolle, J. H. Park, J. C. Meredith and N. Orbey, *ACS Appl. Polym. Mater.*, 2024, **6**, 9430–9439.
6 A. E. Gongora, B. Xu, W. Perry, C. Okoye, P. Riley, K. G. Reyes, E. F. Morgan and K. A. Brown, *Sci. Adv.*, 2020, **6**, eaaz1708.
7 M. Hernández-del Valle, C. Schenk, L. Echevarría-Pastrana, B. Ozdemir, E. Dios-Lázaro, J. Ilarraza-Zuazo, D.-Y. Wang and M. Haranczyk, *Digital Discovery*, 2023, **2**, 1969–1979.
8 B. Stack, M. H. del Valle, A. M. León, L. Langeois and J. Porath, PolyMersion repository, available online: **https://github.com/AMDatIMDEA/PolyMersion**, accessed: 2025-01-08.
9 A. P. Lindvig, UR-RTDE entry in pypi.org, available online: **https://pypi.org/project/ur-rtde/**, accessed: 2024-07-30.
10 A. Touris, A. Turcios, E. Mintz, S. R. Pulugurtha, P. Thor, M. Jolly and U. Jalgaonkar, *Results Mater.*, 2020, **8**, 100149.
11 K. Tanaka, S. Mizuno, H. Honda, T. Katayama and S. Enoki, *J. Solid Mech. Mater. Eng.*, 2013, **7**, 520–529.
12 M. Kurokawa, Y. Uchiyama, T. Iwai and S. Nagai, *Wear*, 2003, **254**, 468–473.
13 B. J. R. Thio and J. C. Meredith, *J. Colloid Interface Sci.*, 2007, **314**, 52–62.
14 ECOPENT®1273 from Cathay Biotech Inc., Datasheet, available online: **https://www.cathaybiotech.com/en/projxags.aspx**, accessed: 2025-04-09.
15 M. Broudin, V. Le Saux, P. Le Gac, C. Champy, G. Robert, P. Charrier and Y. Marco, *Polym. Test.*, 2015, **43**, 10–20.
16 H. Shinzawa and J. Mizukado, *J. Mol. Struct.*, 2020, **1217**, 128389.
17 L. Arboleda-Clemente, A. Ares-Pernas, X.-X. García-Fonte and M.-J. Abad, *J. Mater. Sci.*, 2016, **51**, 8674–8686.
18 M. M. Brette, A. H. Holm, A. D. Drozdov and J. d. C. Christiansen, *Chemistry*, 2024, **6**, 13–50.
19 Ingeo™ Biopolymer 4043D Technical Data Sheet, available online: **https://www.natureworksllc.com//media/Files/NatureWorks/Technical-Documents/Technical-Data-Sheets/TechnicalDataSheet_4043D_3D-monofilament_pdf.pdf**, accessed: 2024-09-10.
20 F. Z. Hosseini, M. Kianifar and M. Azadi, *Polym. Test.*, 2024, **138**, 108562.
21 M. A. Elsawy, K.-H. Kim, J.-W. Park and A. Deep, *Renewable Sustainable Energy Rev.*, 2017, **79**, 1346–1352.
22 N. Yoshikawa, K. Darvish, M. G. Vakili, A. Garg and A. Aspuru-Guzik, *Digital Discovery*, 2023, **2**, 1745–1751.
23 J. Porath and L. Langeois, WaterBathExperiments repository, available online: **https://github.com/AMDatIMDEA/WaterBathExperiments**, accessed: 2025-01-08.